Study of Dispersion and Thermal Stability of V_2O_5/TiO_2-SiO_2 Catalysts by XPS and Other Techniques

Benjaram M. Reddy,* I. Ganesh, and E. Padmanabha Reddy

Inorganic and Physical Chemistry Division, Indian Institute of Chemical Technology, Hyderabad 500 007, India

Received: October 8, 1996; In Final Form: December 13, 1996[⊗]

A high surface area titania−silica binary oxide support was prepared according to the homogeneous precipitation method and was coated with a monolayer of vanadium oxide. The TiO_2-SiO_2 support and the V_2O_5/TiO_2-SiO_2 catalyst were then subjected to thermal treatments from 773 to 1073 K. The influence of heat treatments on the dispersion and thermal stability was investigated by X-ray diffraction, FT infrared, X-ray photoelectron spectroscopy, oxygen uptake, and BET surface area methods. The results suggest that TiO_2-SiO_2 is quite thermally stable even up to 1073 K calcination temperature. However, the V_2O_5/TiO_2-SiO_2 catalyst is stable, in terms of dispersion and surface area, only up to a calcination temperature of 873 K. Thermal treatments beyond this temperature transformed vanadia and titania into crystalline phases and then titania anatase into rutile phase.

Introduction

Catalysts containing vanadium oxide supported on silica, titania, and alumina have been the subject of considerable interest in the recent past due to their successful application in the catalytic oxidation or ammoxidation of hydrocarbons[1−3] and in the selective catalytic reduction (SCR) of nitrogen oxides by ammonia.[4] Although there are other catalysts investigated for the SCR of NO_x, such as platinum, tungsten oxide, molybdenum oxide, iron oxide, and zeolites,[5−8] the vanadium oxide catalysts supported over titania seems to be quite superior to other alternatives due to their high activity and high resistance to poisoning by SO_2. Most of the work in this area has been discussed in detail in a recent review.[8]

Titania in the form of anatase phase is most widely used for SCR purposes, although alumina and to a lesser extent silica are also used. This is primarily because of the remarkable fit of the crystal planes in contact at the vanadia/titania interface, which is assumed to give rise to the epitaxial growth of the vanadia (010) plane at the monolayer level.[9,10] In spite of this advantage, titania as a support suffers from limited surface area, poor mechanical strength, a low sintering resistance, and a high cost. In contrast to TiO_2, the interaction of vanadia with silica is weak and, subsequently, results in a higher tendency for thermally induced agglomeration with a poor dispersion of the active phase,[11] while Al_2O_3 supported V_2O_5 catalysts are susceptible to sulfation.[12]

To overcome the deficiencies of titania, the composite supports containing titania with silica[13−19] or alumina[20−22] have been proposed. In fact, recent studies reveal that TiO_2-SiO_2 is the optimal support for vanadia-based catalysts for NO_x reduction with NH_3, since the composite binary oxide support combines both the mechanical properties of silica and the chemical properties of active titania.[13,16,17]

In addition to De−NO_x purposes the titania−silica mixed oxides are also very interesting materials and find diverse applications. In the glassy state, these materials show zero or negative thermal expansion. Mixed titania−silicas can develop very strong acidity and have been used as acidic catalysts[23] and as supports for ethylene polymerization catalysts. Titania can enter in small amounts under appropriate conditions into the framework of crystalline silica, producing titanium silicate, a very interesting new catalytic material.[24] To increase knowledge on the genesis of the TiO_2-SiO_2 binary oxide and V_2O_5/TiO_2-SiO_2 catalyst system, detailed characterization studies are highly required.

In the present investigation the TiO_2-SiO_2 mixed oxide, obtained *via* a homogeneous precipitation method, and the monolayer V_2O_5/TiO_2-SiO_2 catalyst were subjected to thermal treatments at various temperatures in order to understand the dispersion and thermal stability of these materials. Temperature stability in catalysis is of vital importance, since in high-temperature oxidations or SCR, long-term thermal stability dictates the catalyst life. In this study thermal effects are examined by different characterization techniques including XRD, FTIR, XPS, oxygen uptake, and BET surface area measurements.

Experimental Section

Catalyst Preparation. The titania−silica (1:1 mole ratio) mixed oxide support was prepared by a homogeneous precipitation method using urea as the precipitation reagent. For precipitation with urea, a mixed aqueous solution of titanium tetrachloride (Fluka, AR grade), sodium metasilicate (Loba-Chemie, GR grade), and urea (Loba-Chemie, GR grade) was heated to 368 K with vigorous stirring. Cold $TiCl_4$ was first digested in cold concentrated HCl and subsequently diluted with deionized water, and then Na_2SiO_3, dissolved separately in deionized water, was added. In about 6 h of heating, as decomposition of urea progressed to a certain extent, the formation of precipitate gradually occurred and the pH value of the solution increased. The precipitate was heated for six more hours to facilitate aging. The coprecipitate thus obtained was filtered off and washed thoroughly with doubly distilled water until no chloride ions could be detected with Ag^+ in the filtrate. The obtained cake was then oven dried at 393 K for 16 h. In order to remove sodium ions, the oven-dried precipitates were again washed with ammonium nitrate (Loba-Chemie, GR grade) aqueous solution (5%) and then with hot distilled water several times. The pure $Ti(OH)_4-Si(OH)_4$ coprecipitate thus obtained was oven dried once again at 393 K for 16 h and calcined at 773 K for 6 h in an open-air

* To whom correspondence should be addressed.

[⊗] Abstract published in *Advance ACS Abstracts,* February 15, 1997.

S1089-5647(96)03091-X CCC: $14.00

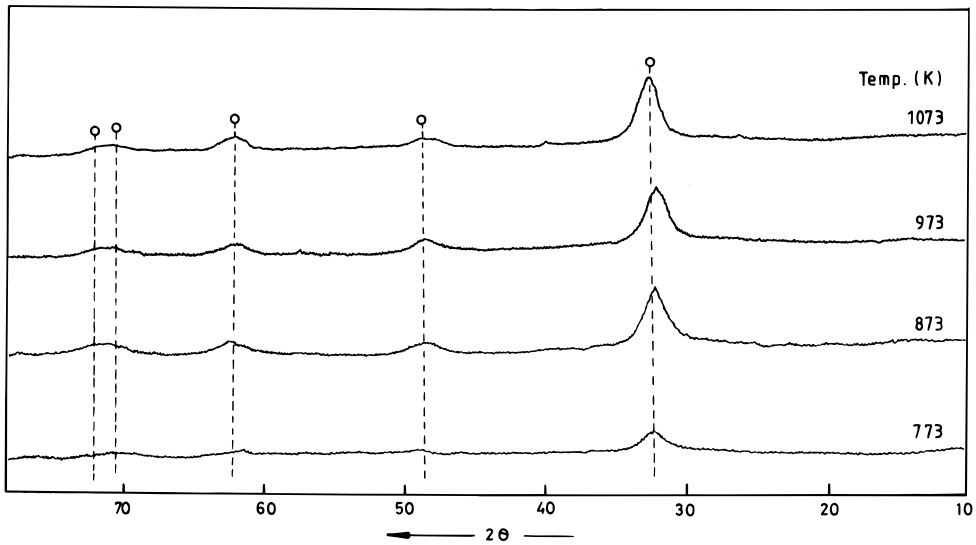

Figure 1. X-ray diffraction patterns of TiO_2-SiO_2 carrier calcined at different temperatures.

atmosphere. Some portions of this support was once again heated at 873, 973, and 1073 K for 6 h in a closed electrical furnace in open-air atmosphere.

The V_2O_5/TiO_2-SiO_2 catalyst, containing 20 wt % V_2O_5, was prepared by a wet impregnation method. To impregnate V_2O_5, the required quantity of ammonium metavanadate (Fluka, AR grade) was dissolved in 1 M oxalic acid (Loba-Chemie, GR grade) solution, and the finely powdered calcined (773 K) support was added to this solution. Excess water was evaporated on a water bath with continuous stirring. The resultant solid was then dried at 383 K for 12 h and calcined at 773 K for 5 h in flowing oxygen. Some portions of the finished catalyst were once again treated at 873, 973, and 1073 K for 6 h in a closed electrical furnace in open-air atmosphere. The rate of heating (as well as cooling) was always maintained at 10 K min^{-1}.

X-ray Diffraction. X-ray diffraction analysis was performed on a Philips PW 1051 diffractometer with nickel filtered CuKα radiation. The XRD phases present in the samples were identified with the help of ASTM Powder Data Files. For comparison purpose, the fraction of rutile in the catalysts was estimated using the following equation

$$X_R = (1 + 0.794I_a/I_r)^{-1}$$

where I_a and I_r are the intensities of (101) and (110) reflections for anatase and rutile, respectively.[18]

Infrared Spectra. The FTIR spectra were recorded on a Nicolet 740 FTIR spectrometer at ambient conditions, using KBr disks, with a nominal resolution of 4 cm^{-1} and averaging 100 spectra.

XPS Measurements. The XPS measurements were made on a VG scientific ESCA Lab II spectrometer (resolution 0.1 eV) with a MgKα source (1253.6 eV). Samples were finely ground and dusted on double-stick Scotch tape on a copper sample holder and covered by a gold mask, and the sample holder was then mounted on the ESCA probe. The scanning of the spectra was done at pressures less than 10^{-8} Torr. Binding energies were measured for O1s, Ti2p, Si2p, V2p, and C1s. The C1s binding energy of 284.6 eV was taken as the standard for correction of experimental binding energies.

Oxygen Uptake and BET Surface Area. A conventional standard static volumetric high-vacuum (1×10^{-6} Torr) system, with the facility for reducing the samples *in situ* by flowing purified hydrogen (35 cm^3 min^{-1}), was used for oxygen uptake measurements. Catalyst samples (*ca.* 0.5 g) were reduced for 4 h at 643 K followed by evacuation at the same temperature for 2 h (1×10^{-6} Torr) prior to O_2 uptake. The amount of O_2 chemisorbed was then determined as the difference between two successive adsorption isotherms obtained at 643 K. Keeping the adsorption temperature constant (643 K), the sample was evacuated for 1 h in between the first and second adsorptions. More details of this method can be found elsewhere.[25] The BET surface area of the catalyst was determined by N_2 physisorption at 77 K on the same standard volumetric high-vacuum system.

Results and Discussion

The titania−silica binary oxide carrier calcined at 773 K had a N_2 BET surface of 238 m^2 g^{-1}. The quantity of vanadia required to cover the support surface as a thin monolayer can be estimated from the area occupied per $VO_{2.5}$ unit[11] of bulk V_2O_5 (0.105 nm^2). However, the maximum amount of vanadium oxide that can be formed as a thin two-dimensional monolayer depends not only on the support surface area but also on the concentration of reactive surface hydroxyl groups. The experimentally determined monolayer capacity of the TiO_2-SiO_2 carrier[19] was found to be 20 wt % V_2O_5. In view of this, a vanadia content of 20 wt % was selected for impregnation in the present investigation.

X-ray diffraction profiles of TiO_2-SiO_2 support and 20% V_2O_5/TiO_2-SiO_2 catalyst calcined at various temperatures are shown in Figures 1 and 2, respectively. In the case of TiO_2-SiO_2 carrier (Figure 1), the diffractogram consists of broad diffraction peaks of TiO_2 anatase (JCPDS Files No. 21-1272), with no evidence of the presence of either rutile (JCPDS Files No. 21-1276) or SiO_2 phase. The anatase peaks are very broad and not well defined, indicating a lack of good crystallinity. However, with increase in calcination temperature there is an increase in the intensity of these peaks indicating an improvement in the crystallinity of the material. A similar improvement in the crystallinity of anatase phase is seen in the case of V_2O_5/TiO_2-SiO_2 catalyst (Figure 2) calcined at 773 K. At 873 K a further improvement in the crystallinity of anatase phase is seen and a partial transformation of anatase into rutile phase starts and crystalline V_2O_5 (JCPDS Files No. 9-387) is also noted. On further raising the calcination temperature to 973 K, the XRD lines due to rutile become very strong with very little presence of anatase phase. A total transformation of anatase into rutile was noted at a calcination temperature of 1073 K.

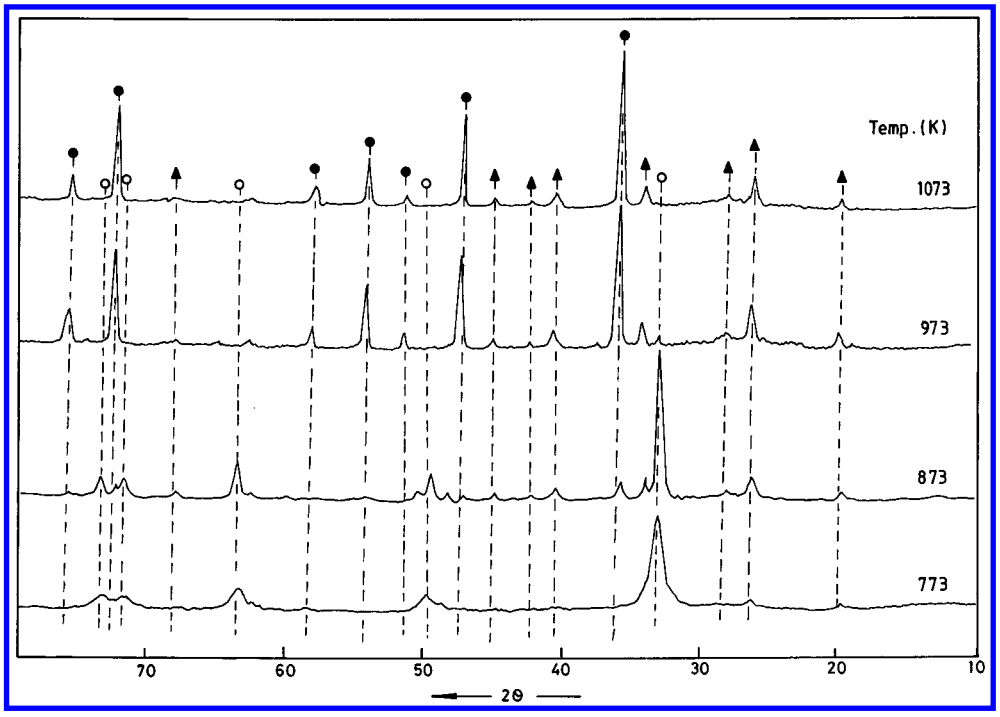

Figure 2. X-ray diffraction patterns of V_2O_5/TiO_2-SiO_2 catalyst calcined at different temperatures: (○) characteristic lines due to anatase phase; (●) lines due to rutile phase; (▲) lines due to V_2O_5 phase.

A closer look at Figures 1 and 2 reveals that the calcination temperature and the vanadium oxide active component are both equally important for the phase transformation phenomena of anatase into rutile. The dispersed vanadia on the TiO_2-SiO_2 support surface appears to lower the activation temperature of the anatase-to-rutile phase transformation, which is normally expected to be 673 K and above in impurity-free TiO_2 samples.[26] It is well-known that at elevated temperatures the supported vanadia phase initiates the anatase-into-rutile phase transformation. During this transformation some of the V_2O_5 is normally reduced and gets incorporated into the rutile structure as $V_xTi_{(1-x)}O_2$ (rutile solid solution).[9,11,27,28] However, in the absence of vanadia, the TiO_2-SiO_2 mixed oxide is quite thermally stable even up to a calcination of 1073 K. In other words, silica when coprecipitated with titania is highly effective in enhancing the thermal stability of titania carrier. Dopants like lanthana, even in small quantities (1−5%), were also found to be highly effective in increasing the thermal stability of TiO_2 anatase recently.[29]

FTIR spectra of TiO_2-SiO_2 carrier and V_2O_5/TiO_2-SiO_2 catalyst calcined at different temperatures are shown in Figure 3. Silica in the absence of titania shows a strong absorption at 1100 cm^{-1}, which is due to Si−O, and another band at 974 cm^{-1} due to O−H bending vibrations of the silinol groups.[30,31] However, in the presence of TiO_2 the bending vibration band shifts to lower frequency and becomes broader with increasing TiO_2 content. This shift of the bending band of the silanol groups to a lower frequency is caused by the interaction between TiO_2 and SiO_2.[31] Anatase and rutile phases of titania exhibit strong absorption bands in the regions of 850−650 and 800−650 cm^{-1}, respectively. With increase in calcination temperature, an increase in the intensity of the band at 1100 cm^{-1} and broadening of the band at 974 cm^{-1} is clearly noted in the case of TiO_2-SiO_2 support (Figure 3a). However, no significant changes with respect to this 1100 cm^{-1} band is seen in the case of V_2O_5/TiO_2-SiO_2 samples (Figure 3b). It is well-known that in the absence of any adsorbed moisture the FTIR spectra of silica give a band at 3740 cm^{-1} due to Si−OH stretching vibrations.[30] In the case of V_2O_5/TiO_2-SiO_2 catalysts calcined

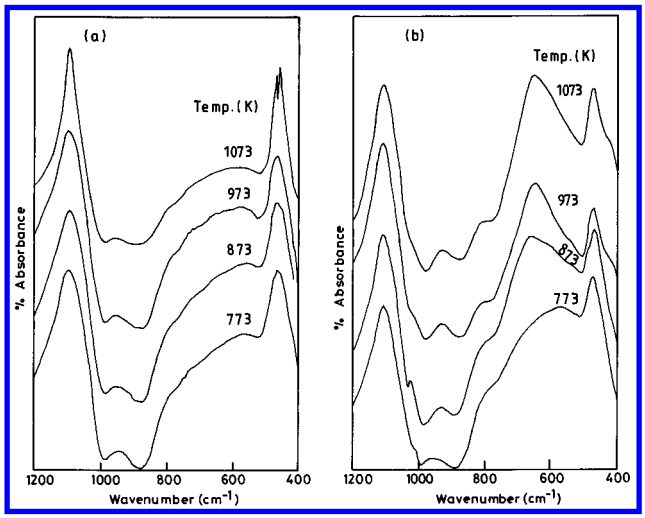

Figure 3. FTIR spectra of various samples calcined at different temperatures: (a) TiO_2-SiO_2; (b) V_2O_5/TiO_2-SiO_2.

at 773 K, the absorption intensity in the −OH stretching vibration region was found to decrease with increase in vanadia content on the support; the intensity for the 30 wt % V_2O_5 catalyst was $^1/_{10}$ the intensity for the support alone.[19] A much similar observation was also made by Bjorklund et al.[32] in agreement with our findings that the vanadia has not reacted with all the Si-OH groups of the carrier. However, no indication for the presence of Ti−OH groups was noted confirming a preferential interaction of vanadia with titania.

The IR spectra of pure V_2O_5 gives sharp bands at 1020 and 825 cm^{-1}, which are due to the V═O stretching and V−O−V deformation modes of vanadium oxide, respectively.[27] In agreement with this argument the FTIR spectra of V_2O_5/TiO_2-SiO_2 samples calcined, especially at 873 K and above, show the presence of some crystalline vanadia. This observation is in perfect agreement with XRD results. As pointed out by Nakagawa et al.[30] for V_2O_5/TiO_2 catalysts, the vanadium oxide on the support surface is normally present as an amorphous two-dimensional vanadia at low vanadium contents and amorphous

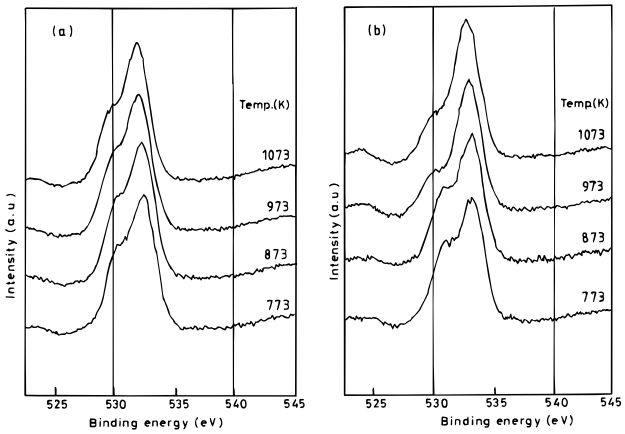

Figure 4. XPS of the O1s binding energy region for various samples calcined at different temperatures: (a) TiO_2-SiO_2; (b) V_2O_5/TiO_2-SiO_2.

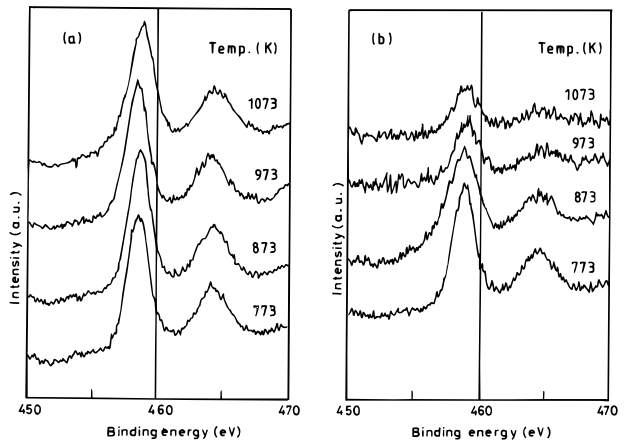

Figure 5. Ti 2p XPS spectra of various samples calcined at different temperatures: (a) TiO_2-SiO_2; (b) V_2O_5/TiO_2-SiO_2.

and crystalline V_2O_5 at higher loadings, i.e., more than monolayer coverages. In our previous study on V_2O_5/TiO_2-SiO_2 and $V_2O_5/TiO_2-Al_2O_3$ catalysts[19,20] calcined at 773 K, we too observed a gradual transformation of an amorphous two-dimensional monolayer vanadia (935−970 cm^{-1}) to a three-dimensional crystalline V_2O_5 with increasing vanadia concentration on the support. The present IR results further show evidence for the phase transformation of titania anatase into rutile with increase in calcination temperature. In line with XRD observations, the FTIR results also confirm that the interaction of V_2O_5 with TiO_2 is stronger than that of SiO_2. The mutual interaction between V_2O_5 and TiO_2 weakens the interaction of vanadia and titania with the silica resulting in the formation of their crystalline phase.[19] This observation is further supported by ESCA results presented in the paragraphs below.

The samples of TiO_2-SiO_2 and V_2O_5/TiO_2-SiO_2 calcined at different temperatures are investigated by ESCA. The XPS bands of O1s, Ti2p, Si2p, and V2p are shown in Figures 4−7, respectively, and the corresponding binding energies and the intensity ratios are summarized in Table 1. For the purpose of better comparison, the XPS bands of O1s, Ti2p pertaining to the TiO_2-SiO_2 carrier are shown in Figures 4a, 5a, and 6a, and the corresponding bands of V_2O_5/TiO_2-SiO_2 catalyst are presented in Figures 4b, 5b, and 6b, respectively. These figures clearly indicate that the XPS bands depend on the particle size (influenced by calcination temperature) and the coverage of vanadium oxide on the carrier in agreement with the literature.[13,33−36] As shown in Figure 4a, the O1s profile is, in general, more complicated due to the overlapping contributions of

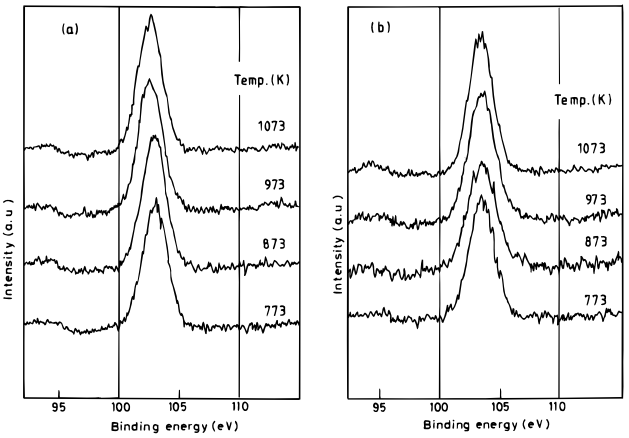

Figure 6. Si 2p XPS spectra of various samples calcined at different at different temperatures: (a) TiO_2-SiO_2; (b) V_2O_5/TiO_2-SiO_2.

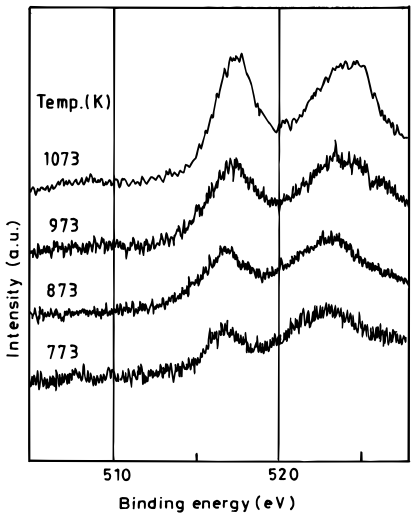

Figure 7. V2p XPS spectra of V_2O_5/TiO_2-SiO_2 catalysts calcined at different temperatures.

TABLE 1: Binding Energies and XPS Intensity Ratios of TiO_2-SiO_2 and V_2O_5/TiO_2-SiO_2 Samples Calcined at Different Temperatures

			Ti					
temp (K)	O1s	$Si2p_{1/2}$	$2p_{1/2}$	$2p_{3/2}$	$V2p_{3/2}$	I_{Ti}/I_{Si}	I_V/I_{Ti}	I_V/I_{Si}
TiO_2-SiO_2 Samples								
773	532.3	103.1	464.3	458.3		0.930		
873	532.2	102.9	464.5	458.5		0.948		
973	531.9	102.7	464.4	458.4		0.947		
1073	531.8	102.7	464.6	458.6		0.920		
V_2O_5/TiO_2-SiO_2 Samples								
773	532.8	103.5	464.5	458.8	516.8	0.910	0.333	0.303
873	532.7	103.5	464.6	458.7	516.9	0.700	0.513	0.358
973	532.8	103.6	464.7	458.5	517.3	0.476	0.962	0.451
1073	532.9	103.4	464.5	458.6	517.8	0.340	1.846	0.621

oxygen from silica and titania and whose origin lies in the MgKα. Two oxygen peaks are mainly observed for both the series of samples in agreement with the literature. It is known that the intense peak at higher binding energy belongs to the oxygen atoms that are more strongly bound to Ti (e.g. TiO_2) and the one at lower binding energy belonging mainly to Si, judging from the difference in the electronegativity of the elements.[37] The unresolved shoulder peak imposed on the O1s intense peak for TiO_2-SiO_2 support is due to the Ti-rich domain.[38] In the case of TiO_2-SiO_2 carrier, the binding energy of the most intense O1s peak (Table 1) decreased with increase in calcination temperature. However, no such decrease was observed in the case of V_2O_5/TiO_2-SiO_2 catalysts.

Figure 5 shows the binding energies of the Ti2p core levels, found at 458.5 and 464.5 eV for $Ti2p_{3/2}$ and $2p_{1/2}$ lines, respectively, which agree well with the values previously reported in the literature.[39] Very interestingly, the intensity of the Ti2p core level spectra decreased with increasing calcination temperature. This decrease in the intensity is more pronounced (Figure 5b) in the case of V_2O_5-impregnated TiO_2-SiO_2 samples. It is also evident from Figure 5 that the intensity of Ti2p photoelectron signals depend on the calcination temperature as well as on the coverage of vanadium oxide on titania−silica carrier. Figure 6 shows the binding energy of the $Si2p_{1/2}$ core level found around 103 eV, which agrees well with the values reported in the literature.[36] Here again the intensity of the spectra decreases with increasing calcination temperature, and this decrease is more predominant in the case of V_2O_5/TiO_2-SiO_2 catalysts. Table 1 lists the Ti:Si intensity ratios for TiO_2-SiO_2 support. This ratio remains unchanged with increase in calcination temperature. This ratio was, however, found to decrease with increase in calcination temperature in the case of V_2O_5/TiO_2-SiO_2 samples. It may, therefore, be suggested that titania−silica mixed oxide support is quite thermally stable in the absence of vanadium oxide on its surface. The XPS results observed in the case of TiO_2-SiO_2 support are in perfect agreement with the results of XRD and FTIR.

Figure 7 shows the binding energy and the intensity of $V2p_{3/2}$ line which increased with increasing calcination temperature. At 773 K calcination the binding energy of $V2p_{3/2}$ was 516.6 eV; it probably corresponds to the V^{IV} state. With increasing calcination temperature (773−1073 K), the binding energy of $V2p_{3/2}$ increases from 516.6 to 517.8 (Table 1), an indication of increase in the oxidation state of vanadium.[33] This increase in oxidation state of vanadium is primarily due to increasing the crystalline vanadium oxide on the support surface. Vanadia in the tetravalent state is stabilized by the presence of titania anatase phase in the amorphous TiO_2-SiO_2 mixed oxide support. As the calcination temperature increased, the crystalline rutile phase of titania occurs, thereby decreasing the proportion of amorphous material, and the pentavalent state of vanadia is stabilized. From these data it is clear that the binding energy of the $V2p_{3/2}$ peak depends on the type of carrier and can be explained as due to the substrate, which depends markedly on the electronic environment and coordination of the surface sites.[33]

The relative dispersion of vanadium on the support surface was also estimated from the XPS measurements of 20% V_2O_5/TiO_2-SiO_2 catalyst calcined at different temperatures. The intense signal corresponding to the $V2p_{3/2}$ level of vanadium was measured and compared with Si2p and $Ti2p_{3/2}$ levels. The V2p/Ti2p and V2p/Si2p ratios were taken as a measure of the relative dispersion of vanadium oxide on the support surface as shown in Figure 8. The precise determination of binding energy is difficult because of the O1s satellite interfering peak, whose origin lies in the MgKα line. This fact has been well documented in the literature.[40] The resolution of the $V2p_{1/2}$ level is much poorer than that of the $V2p_{3/2}$ level. Consequently, only the $V2p_{3/2}$ was considered in the calculations. In the case of V_2O_5/TiO_2-SiO_2 catalysts the Ti:Si intensity ratio decreased with increasing calcination temperature; however, in the case of pure support it remained unchanged (Table 1). It may be due to the phase transformation of titania from anatase to rutile at higher calcination temperatures in the presence of vanadium oxide on its surface. The V:Si intensity ratio is almost equal to the V:Ti intensity ratio (Figure 8) for V_2O_5/TiO_2-SiO_2 catalyst at 773 K, but at 1073 K the V:Si intensity ratio was three times lower than the V:Ti intensity ratio. The difference between V:Si and V:Ti intensity ratios increases with increase in the calcination temperature. From these data it is clear that the interaction between vanadia and silica is weaker than the interaction between vanadia and titania. The IR observation of Si−OH free groups[19] also supports this finding. The XPS intensity ratios of V:Ti and V:Si for V_2O_5/TiO_2-SiO_2 indicate further that a good degree of dispersion of vanadium occurs at lower calcination temperature, but with increasing calcination temperature the dispersion of vanadium decreases. When calcination temperature increases, dispersed vanadium oxide species condense and crystallize as V_2O_5 forming multilayers onto the TiO_2 surface, and obviously, the dispersion of vanadium decreases. This behavior clearly explains the greater increase of the V:Ti ESCA intensity ratio than the V:Si ratio.

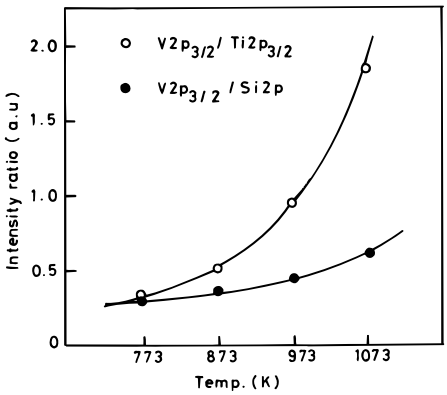

Figure 8. XPS intensity ratio *versus* calcination temperature for V_2O_5/TiO_2-SiO_2 catalysts.

TABLE 2: BET Surface Area and Dispersion of Vanadium as a Function of Calcination Temperature

	TiO_2-SiO_2 carrier	V_2O_5/TiO_2-SiO_2 catalyst	
temp (K)	$S_{BET/m2g-1}$	$S_{BET/m2g-1}$	D^a
773	238	125	0.83
873	227	41	0.77
973	189	12	0.26
1073	172	5	0.23

[a] Dispersion = fraction of vanadium atoms at the surface assuming $O_{ads}/V_{surf} = 1$.

The N_2 BET surface areas of titania−silica support and the vanadia−titania−silica catalyst calcined at different temperatures are shown in Table 2. As can be noted from this table, the BET surface area in both cases decreases with increase in calcination temperature. However, in the case of the TiO_2-SiO_2 carrier the decrease is less when compared to the V_2O_5/TiO_2-SiO_2 catalyst. These results are in line with XRD, IR, and ESCA observations, which unequivocally state that the vanadia preferentially interacts with titania and induces the so-called phase transformation of titania−anatase into rutile and is accelerated by calcination temperature. The high-temperature calcination induces the crystallite growth and hence a substantial loss in the surface area.

The dispersion of vanadium oxide on the TiO_2-SiO_2 support as a function of calcination temperature is also presented in Table 2. This dispersion was estimated from the oxygen uptake measurements obtained at 643 K on the prereduced catalysts at the same temperature. Here, the dispersion is defined as the ratio of molecular oxygen uptake to V_2O_5 content[41] ($O_2/V_2O_5 = 1$). The pure TiO_2-SiO_2 support was also found to chemisorb some small amount of O_2 under the experimental conditions used in this study. Therefore, the contribution of the support alone was subtracted from the results. As can be noted from Table 2, the apparent dispersion decreases with

increase in calcination temperature. This decrease is more predominant in the case of catalysts calcined at 973 and 1073 K. As described earlier, some of the vanadia is normally reduced and forms, with the titania support, a solid solution when calcined at elevated temperatures.[9,11,27,28] However, for the calcinations at 773 and 873 K the dispersion remains high. Thus, the dispersion values obtained from oxygen uptake measurements are in line with XRD, FTIR, and ESCA observations.

Determination of dispersion of the active component on a carrier is one of the best ways of characterizing a supported catalyst. The dispersion of metal catalysts is normally determined by the selective chemisorption of H_2 and to some extent CO at appropriate conditions. The quest for a similar method for metal oxide systems lead to the development of simple low-temperature oxygen chemisorption (195 K) for supported molybdenum and vanadium catalysts by various groups.[42−44] The recent study by Oyama et al.[41] emphasized the significance of temperature of reduction as well as uptake and showed that at around 640 K sample reduction followed by O_2 chemisorption would yield more meaningful information in the case of V_2O_5/SiO_2 catalysts. The modified volumetric version of this method was also found to give valuable information about the dispersion of vanadium oxide on various supports other than SiO_2.[19,20,25,45] From the present study the dispersion trends observed from O_2 uptake measurements are in line with the results obtained from other techniques. The vanadium oxide dispersions generated from O_2 uptake measurements were also found to correlate well with the results of ESR[46], solid state ^{51}V NMR, and other methods.[47,48]

Conclusions

The following conclusions can be drawn from this study: (1) The TiO_2-SiO_2 mixed oxide is a promising support as well as a catalyst. It is thermally quite stable even up to a calcination temperature of 1073 K in the absence of vanadium oxide or any other impurities. The titania−silica binary oxide mainly contains two titania phases: an amorphous phase containing probably isolated Ti-sites tetrahedrally coordinated by Si−O and OH groups and a segregated paracrystalline TiO_2 (anatase or rutile). This phase distribution is highly sensitive to calcination temperature and vanadium oxide content. (2) Highly dispersed vanadium oxide monolayer catalysts with vanadia loadings nearly equivalent to the theoretical monolayer capacity of the support material can be obtained with TiO_2-SiO_2 mixed oxide as the carrier. (3) The amorphous anatase titania in V_2O_5/TiO_2-SiO_2 catalyst undergoes crystallization and subsequent phase transformation into rutile when subjected to thermal treatments beyond 873 K temperatures.

Acknowledgment. Thanks are due to CSIR and UGC, New Delhi, for the award of research associateship and junior research fellowship to E. P. R. and I. G., respectively.

References and Notes

(1) Hucknall, D. J. *Selective Oxidation of Hydrocarbons*; Academic Press: New York, 1974.
(2) Bond, G. C.; Tahir, S. F. *Appl. Catal.* **1991**, *71*, 1 and references therein.
(3) Reddy, B. N.; Reddy, B. M.; Subrahmanyam, M. *J. Chem. Soc., Faraday Trans.* **1991**, *81*, 1655.
(4) Wong, W. C.; Nobe, K. *Ind. Eng. Chem. Prod. Res. Dev.* **1984**, *23*, 564.
(5) Andersson, L. A. H.; Brandin, J. G. M.; Odenbrand, C. U. I. *Catal. Today* **1989**, *4*, 187.
(6) Wong, W. C.; Nobe, K. *Ind. Eng. Chem. Prod. Res. Dev.* **1986**, *25*, 179.
(7) Okazaki, S.; Kumasaka, M.; Yoshida, Y.; Ksaka, K.; Tanabe, K. *Ind. Eng. Chem. Prod. Res. Dev.* **1981**, *20*, 301.
(8) Bosch, H.; Janssen, F. *Catal. Today*, **1988**, *2*, 369.
(9) Vejux, A.; Courtine, P. *J. Solid State Chem.* **1978**, *23*, 93.
(10) Reddy, B. M.; Reddy, E. P.; Mehdi, S. *Mater. Chem. Phys.* **1994**, *36*, 267.
(11) Roozeboom, F.; Mittlemeijer-Hazeleger, M. C.; Moulijn, J. A.; Medema, J.; de Beer, V. H. J.; Gellings, P. J. *J. Phys. Chem.* **1980**, *84*, 2783.
(12) Shikada, T.; Fujimoto, K.; Kunugi, T.; Tominaga, H.; Kaneko, S.; Kubo, Y. *Ind. Eng. Chem. Prod. Res. Dev.* **1981**, *20*, 91.
(13) Galan-Fereres, M.; Mariscal, R.; Alemany, L. J.; Fierro, J. L. G.; Anderson, J. A. *J. Chem. Soc., Faraday Trans.* **1994**, *90*, 3711.
(14) Reichmann, M. G.; Bell, A. T. *Appl. Catal.* **1987**, *32*, 315.
(15) Vogt, E. T. C.; Boot, A.; van Dillen, A. J.; Geus, J. W.; Janssen, F. J. J. G.; van der Kerkhof, F. M. G. *J. Catal.* **1988**, *114*, 313.
(16) Baiker, A.; Dollenmeier, P.; Glinski, M.; Reller, A. *Appl. Catal.* **1987**, *35*, 365.
(17) Hany, B. E.; Baiker, A.; Schrami-Murth, M.; Wakaun, A. *J. Catal.* **1992**, *133*, 1.
(18) Wauthoz, P.; Ruwet, M.; Machej, T.; Grange, P. *Appl. Catal.* **1991**, *69*, 149.
(19) Reddy, B. M.; Mehdi, S.; Reddy, E. P. *Catal. Lett.* **1993**, *20*, 317.
(20) Reddy, B. M.; Kumar, M. V.; Reddy, E. P.; Mehdi, S. *Catal. Lett.* **1996**, *36*, 187.
(21) Clarebout, G.; Ruwet, M.; Matralis, H.; Grange, P. *Appl. Catal.* **1991**, *76*, L9.
(22) Matralis, H. K.; Ciardelli, M.; Ruwet, M.; Grange, P. *J. Catal.* **1995**, *157*, 368 and references therein.
(23) Odenbrand, C. U. I.; Brandin, J. G. M.; Busca, G. *J. Catal.* **1992**, *135*, 505.
(24) Taramasso, M.; Perego, G.; Notari, B. U.S. Patent 4,410,501, 1983.
(25) Reddy, B. M.; Manohar, B.; Reddy, E. P. *Langmuir* **1993**, *9*, 1781.
(26) Yoganarasimhan, S. R.; Rao, C. N. R. *Trans. Faraday Soc.* **1962**, *58*, 1579.
(27) Bond, G. C.; Sarkany, A.; Parfitt, G. D. *J. Catal.* **1979**, *57*, 476.
(28) Kozlowski, R.; Pettifer, R. F.; Thomas, J. M. *J. Phys. Chem.* **1983**, *87*, 5176.
(29) Le Duc, C. A.; Campbell, J. M.; Rossin, J. A. *Ind. Eng. Chem. Res.* **1996**, *35*, 2473.
(30) Nakagawa, Y.; Ono, O.; Miyata, H.; Kubokawa, Y. *J. Chem. Soc., Faraday Trans.* **1983**, *79*, 2929.
(31) Sohn, J. R.; Jang, H. J. *J. Catal.* **1991**, *132*, 563.
(32) Bjorklund, R. B.; Odenbrand, C. V. I.; Brandin, J. G. M.; Andersson, L. A. H.; Liedberg, B. *J. Catal.* **1989**, *119*, 187.
(33) Nag, N. K.; Massoth, F. E. *J. Catal.* **1990**, *124*, 127.
(34) Johson, B.; Rebenstrof, B.; Larsson, R.; Andersson, S. L. T. *J. Chem. Soc., Faraday Trans.* **1988**, *84*, 1897.
(35) Chiarello, G.; Robba, D.; De Michele, G.; Parmigiani, F. *Appl. Surf. Sci.* **1993**, *64*, 91.
(36) Odenbrand, C. U. I.; Andersson, S. L. T.; Andersson, L. A. H.; Brandin, J. M. G.; Busca, G. *J. Catal.* **1990**, *125*, 451.
(37) Imamura, I.; Ishida, S.; Taramoto, H.; Saito, Y. *J. Chem. Soc., Faraday Trans.* **1993**, *89*, 757.
(38) Greegor, R. B.; Lytle, F. W.; Standstorm, D. R.; Wong, J.; Schultz, P. *J. Non-Cryst. Solids*, **1983**, *55*, 27.
(39) Sawatzky, G. A.; Post, D. *Phys. Rev.* **1979**, *B20*, 1546.
(40) Gil-Llambias, F. J.; Escuday, A. M.; Fierro, J. L. G.; Lopez Agudo, A. *J. Catal.* **1985**, *95*, 520.
(41) Oyama, S. T.; Went, G. T.; Bell, A. T.; Somorjai, G. A. *J. Phys. Chem.* **1989**, *93*, 6789.
(42) Parekh, B. S.; Weller, S. W. *J. Catal.* **1977**, *47*, 100.
(43) Nag, N. K.; Chary, K. V. R.; Reddy, B. M. Rao, B. R.; Subrahmanyam, V. S. *Appl. Catal.* **1984**, *9*, 225.
(44) Fierro, J. L. G.; Gambaro, L. A.; Cooper, T. A.; Kremen, G. *Appl. Catal.* **1983**, *6*, 363.
(45) Reddy, B. M. *Catalytic Selective Oxidation*; ACS Symposium Series 523; Oyama, S. T., Hightower, J. W., Eds.; American Chemical Society: Washington, DC, 1993; p 204.
(46) Chary, K. V. R.; Reddy, B. M.; Nag, N. K.; Subrahmanyam, V. S.; Sunandana, S. *J. Phys. Chem.* **1984**, *88*, 2622.
(47) Narsimha, K.; Reddy, B. M.; Rao, P. K.; Mastikhin, V. M. *J. Phys. Chem.* **1990**, *94*, 7336.
(48) Reddy, B. M.; Reddy, E. P.; Srinivas, S. T.; Mastikhin, V. M.; Nosov, A. V.; Lapina, O. B. *J. Phys. Chem.* **1992**, *96*, 7076.